Numerical Simulation of Cracked Reinforced Concrete Slabs Subjected to Blast Loading

Zhang Wenjiao [a*], Kong Xiangqing [a], Qu Yandong [a], Zhao Qian [a]

[a] *Department of Civil & Architectural Engineering, Liaoning University of Technology, Jinzhou, 121001, China.*

Abstract

Crack is one of the most common defects observed in reinforced concrete (RC) structures. An initial crack will lead to severe changes in the stress state when the structure subjected to blast loadings. Target on acquiring the dynamic data, a finite element method is applied to simulate the response of cracked RC slab subjected to blast loading. The theoretical results of damage distribution and mid-span deflection of normal specimens are first compared with experimental test, which indicates that the dynamic behaviour of RC slab under blast loading can be well predicted by the finite element model. Then blast responses of cracked RC slabs with varied crack parameters (e.g. orientation, width and depth) are systematically studied. Results show that damage of the cracked slab initiates from the initial crack tip of the bottom surface, and then it propagates quickly with cracks found in the support areas on the top surface. In addition, the existence of initial cracks in the RC slab make it subject to more serious damages than the normal RC slab under the same explosive loads, as well as a short reacted failure time. Moreover, variations of crack parameters have slight influences on the distributions of cracked RC slab.

Keywords: Blast Loading; Cracked RC Slab; Dynamic Behaviour; Damage Distribution; Mid-span Deflection.

1. Introduction

Reinforced concrete is a principal construction material used for civil buildings. During their serving life, these structures might be subjected to extreme loadings, such as blast loadings due to terrorist bombing or accidental gas explosion. The strength of blast loadings are much higher than that of the conventional loadings, so blast loading can prominently influence the structural response. The behaviour of reinforced concrete (RC) structure remains as one of the largest sources of uncertainty in civil engineering, even though a tremendous amount of research work has been carried out on this issue [1-3]. Generally, most of the uncertainties are due to the lack of understanding of the deformation, strains and stresses in the RC members during instant loading. It is therefore important to study the response of RC structures under blast loading to provide reliable design guidelines to resist blast loading.

As one of the main bearing components of RC structure commonly used in protective design against potential blast loading conditions, dynamic analysis of RC slab has important significance in antiknock design and reinforcement for building structure. The current analysis method for RC components, especially RC slabs subjected to blast loading, mainly consists of two major aspects, experimental and numerical studies. Various experimental studies on the reinforced concrete panels subjected to blast loading have been reported. Razaqpur et al. conducted a test of clamped reinforced concrete panels subjected to explosive loading [4]. Mays et al. investigated the dynamic response of a simply supported reinforced concrete panels with openings under blast loading [5]. Sun studied the blast test on a simply supported one-way reinforced concrete panel [6]. Lok and Xiao investigated the air blast tests on steel fiber

---

reinforced concrete panels with various fiber types and boundary conditions [7]. In addition, Chi et al. investigated the blast responses of sandwich panels consisting of mild steel face plates and aluminium honeycomb cores. However, full scale experimental test is usually costly and time consuming. Numerical study is another commonly used method and has been widely adopted for investigating the structural dynamic response to blast loading [8]. Xu and Lu proposed a 3D finite element model using LS-DYNA for modelling reinforced concrete plates subjected to blast loading and investigated different levels of damages in concrete [9]. Yuan et al. carried out a numerical simulation of contact detonation on a concrete slab and discussed the dynamic response, damage distributions and effect of reinforcing bars on anti-spallation capability of the concrete slabs [10]. Tai et al. performed numerical study on the dynamic response of RC structures under explosive loading, and investigated the destruction of RC slabs with different parameters [11]. Zhao and Chen investigated the dynamics response and damage mechanism of three reinforcement concrete slabs subjected to close-in explosions using LS-DYNA software and compared that with experimental tests [12]. Lin et al. simulated the damage process of RC panels subjected to blast loading with LS-DYNA, and investigated the effects of explosive mass, standoff distance, panel thickness and reinforcement ratio on the blast resistance of RC panels [13]. Wang et al. studied the behaviour of one-way square RC slabs subjected to blast loading through both experiments and numerical simulations [14].

It is noticed from the above literature review, studies of blast response of RC slabs are mainly focused on normal structures without any defects. Actually, initial crack is one of the most common defects observed in member, which will make the bearing capacity of the member significantly decreased and even lead to the destruction of the whole structures. A great deal of attention has focused in recent decades on the structural performance of the cracked member and much effort has been devoted to researching this hot topic. For instance, Brighenti performed a numerical study on the buckling behaviour of thin cracked plates under tension, compression and shear loading, and investigated the effects of the boundary condition, crack length and orientation on the buckling collapse of the plates [15]. Paik et al. carried out experimental and numerical studies on the ultimate strength of cracked steel plate subjected to axial compressive or tensile loads, and estimated the ultimate strength reduction characteristics of plate elements due to cracking damage with varying sizes and locations [16]. Hao et al. conducted experimental investigations on the fatigue behaviour of thick center cracked aluminum plates bonded with two-sided composite patches [17]. Alinia used the finite element method to analyze shear panels including central or edge cracks [18].

Although previous studies have made great progress in the structural behaviour of cracked slabs, most of them are mainly focused on that with consideration of being subjected to static loads. Limited work has been conducted on the dynamic response of cracked slabs, especially the cracked RC slabs subjected to blast loadings. Therefore, in this paper, a series of numerical studies are conducted aiming to get a dynamic data of the cracked RC slabs under blast loading by using a nonlinear finite element method based on the commercial software package LS-DYNA [19]. The finite element model is firstly calibrated based on previous experimental test results as reported by Sun [6]. Intensive simulations are then carried out using the calibrated numerical model to identify the blast response of the RC slab with an initial crack in the center of the bottom surface, by comparing the damage distribution and maximum deflection of the cracked specimens with that of the normal (un-cracked) models. Based on the numerical simulation results, influences of different crack parameters (e.g. orientation, width and depth) on dynamic behaviour of the cracked RC slabs subjected to air blast loading are revealed.

2. Numerical Model Calibration

In this paper, the commercial finite element code LS-DYNA is adopted to study the whole process through its explicit time integration scheme. LS-DYNA has the capability of simulating large-strain effect for the solid materials when subjected to high velocity impact and blast loading. It has been proved to be capable of yielding reliable numerical predictions of structural response and damage to blast loading.

2.1. Experimental Descriptions

Experimental tests conducted by Sun in 2009 are used for the validation of the numerical simulation. Dynamic responses of RC slabs to the blast loading are simulated. The simulated results of damage distribution and mid-span deflection of RC slabs with no defect are compared with those recorded in the test [6]. Due to the few information of blasting test on cracked RC slabs can be get in the open literature, testing data conducted on normal (un-cracked) RC slabs without crack is adopted to verify the numerical model in the present study. Researches show that the dynamic response of RC structures under air blast loading mainly depends on properties of the concrete material as well as the reinforced confinements, not structure types and boundary conditions [20-21]. So it is believed that the numerical model calibrated is applicable to simulating blast responses of cracked RC slabs as the same material properties that of the normal RC slab.

The test setup is shown in Figure 1, a one-way reinforced concrete slab with size of 1300×1000×120 mm (length × width × height) was tested to study the dynamic response of RC structure under blast loading. The thickness of concrete cover is 25 mm. Longitudinal reinforcements include 11 steel bars of Φ10-HPB235 while 8 steel bars of Φ10-

HPB235 bars are used for transverse reinforcements. The concrete has an average compressive strength of 48 MPa, and the reinforcement has the yield strength of 560 MPa and a Young's modulus of 230 GPa. The RC slab is placed on a steel frame, and the two short sides of RC slab are clamed to prevent uplifting during the test. Four wooden blocks are placed between the steel frame and the specimen to avoid stress concentration on the specimen edges. The blast loading is generated by the detonation of 2.09 kg trinitrotoluene (TNT) explosive charges located at a 600 mm standoff above the specimen in the test. More detailed information of the tested slab can be found in Sun (2009) studies [6].
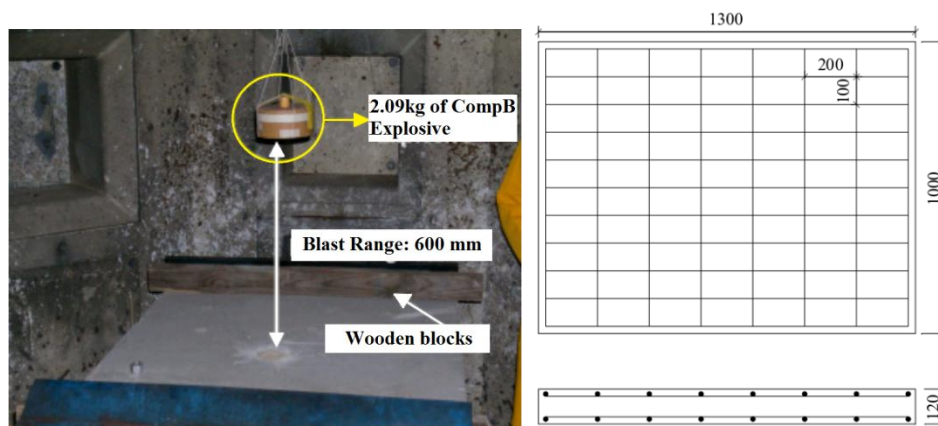

Figure 1. Experiment setup [6]

2.2. Numerical Model

2.2.1. Finite Element Model, Boundary Conditions

Analysis conducted in this paper involves simulating has the same size of RC slab as stated above. As shown in Figure 2, RC slab is supported on two rigid plates, which are made of solid elements to simulate the experimental conditions. The concrete slab is modelled using SOLID 164 element which is an 8-node constant stress hexahedron brick element. Steel reinforcement bars are modelled using BEAM 161. Considering the convenience of modelling, force checking and short time-consuming, no slip between the steel reinforcement and concrete is assumed. However, in real cases, bond-slip between steel and concrete is exist, and it is found that the perfect bond assumption has fewer influence to the result of RC structures under blast loading [13, 22, 23]. The Lagrangian formulation in which the coordinates move with the material is applied in the analysis.

A proper grid size can properly reduce the computation time and ensure the accuracy. After verifying the convergence of the grid, element size of the concrete and steel is defined as 5×5 mm, typical finite element meshes are shown in Figure 2b. The total element number for the normal RC slab is 20,800 whereas the element number 904 is used for the steel reinforcement. The axial symmetry with respect to the central line of the RC slab is assumed, thus only 1/4 of the slab is modelled to reduce the computation time. 2.09 kg TNT charge was placed at 600 mm away from the centre of the reinforced concrete slab.

Constraints are defined to be fixed on the support plates, so that it cannot translate but will be able to rotate about its own longitudinal axis. Models of reinforced concrete slab with long edge are free, while the two short edges are constrained its vertical displacement to prevent the concrete panel from bouncing back up.
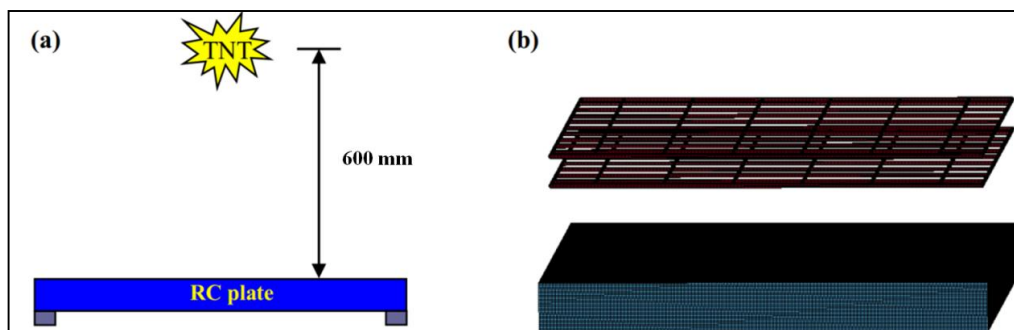

Figure 2. (a) Finite element model; (b) Concrete and reinforcing steel meshing

2.2.2. Material Model

In LS-DYNA, various material models can be used to simulate the dynamic response of a reinforced concrete structure to blast loading, such as Soil and Foam Model (Mat_5), Pseudo-Tensor (Mat_16), Orientated Crack (Mat_17), Geological Cap (Mat_25), Concrete Damage (Mat_72), Concrete Damage Rel3 (Mat_72_REL3), Brittle

Damage (Mat_96), Soil Concrete (Mat_78), Winfrith Concrete (Mat_84), Johnson Holmquist Concrete (Mat_111). Some of the models take into account the pressure hardening, strain hardening and strain rate dependency of concrete material, while some of these models are limited to a certain class of problems due to their highly restrictive assumptions [24].

An appropriate material model for concrete is vital for the reliable simulation of RC structure subjected to blast loading. In this study, the material model *Mat Concrete Damage Rel3 (MAT_72_REL3) is used to simulate the concrete material. This material model is the third release of Karagozian and Case (K&C) concrete model which is a plasticity-based model using three shear failure surfaces and including damage and strain-rate effect. Different dynamic increase factors (DIFs) which will be introduced in the following paragraph can be applied for concrete in tension and compression to simulate the desired rate effect in this model. The strategy used in fitting the strain softening can be modified automatically when parameters for generic concrete material were input the model [25], which makes it relatively simple and numerically robust compared with other constitutive models used for concrete-like materials. It can reproduce key concrete behaviours which are vital to blast analyses, and it is also easy to be calibrated using laboratory data [26].

In this model, three independent strength surfaces, i.e., initial yield surface, maximum failure surface and residual surface are used to describe the plastic properties of concrete, the strength surface is defined as [26]:

$$\Delta\sigma_i = a_{0i} + p/(a_{1i} + a_{2i} \times p) \tag{1}$$

Where $\Delta\sigma_i$ is the ith failure surface, a_{0i}, a_{1i} and a_{2i} are the parameters which can be determined from laboratory data in unconfined compression tests and conventional triaxial compression tests at a range of confining pressures, and $p = -(\sigma_x + \sigma_y + \sigma_z)/3$ is the hydrostatic pressure (stresses are positive in tension, pressure is positive in compression), in which σ_x, σ_y and σ_z are the principal stresses.

After reaching the initial yield surface but before the maximum failure surface, the current plasticity surface is obtained as a linear interpolation between the two, which means the concrete is at a hardening stage. While after reaching the maximum surface, the current failure surface is similarly interpolated between the maximum and the residual, as the concrete is at a softening stage.

The maximum failure surface for concrete is related to the concrete compressive strength fc, which can be expressed as [25]:

$$\frac{\Delta\sigma}{f_c} = a_0 + \frac{p/f_c}{a_1 + \frac{a_2 p}{f_c}} \tag{2}$$

Where $\Delta\sigma = \sqrt{3J_2}$ is the failure surface for the deviatoric stresses, in which $J_2 = \sqrt{s_1^2 + s_2^2 + s_3^3}$ is the second invariant of the deviatoric stress tensor, and s_1, s_2 and s_3 are the principal deviatoric stresses.

In LS-DYNA, the EOS Tabulated Compaction (EOS 8) which gives the current pressure as a function of the volumetric strain is used together with MAT_72_R3, the equation of volumetric strain is expressed as [19]:

$$p = C(\varepsilon_v) + \gamma T(\varepsilon_v)E \tag{3}$$

Where ε_v is the volume strain which is given by the natural logarithm of the relative volume. γ is the ratio of specific heats. C and T are coefficients given as the functions of ε_v, and E the internal energy.

As shown in Figure 3, compaction of the concrete occurs when the volumetric strain exceeds the elastic limit, and tensile failure occurs when the tension stress is greater than the hydrostatic tension. The volumetric strain affects the bulk unloading modulus. When the pressure is cut-off, unloading goes along the unloading bulk modulus. When the sample is reloaded again, reloading follows the unloading path to the point where unloading begins, and continues on the loading path.

Previous studies [27-30] have shown that the model of MAT_72_REL3 is reliable to predict the response of reinforced concrete structure subjected to blast loading. The material parameters of

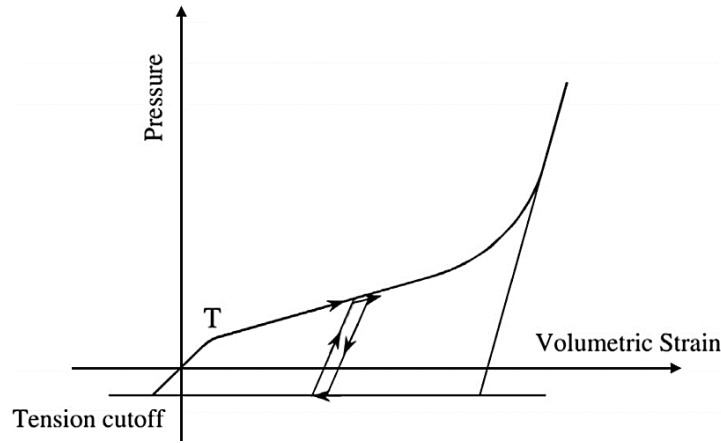Concrete used in this paper are shown in Table 1 [6, 31].

Figure 3. Pressure versus volumetric strain curve for EOS 8 [19]

Table l. Material parameters of concrete and steel reinforcement [6, 31]

Material	LS-DYNA Model	Input parameter	Magnitude
Concrete	*MAT_CONCRETE_DAMAGE_REL3 (MAT_72_REL3)	Mass density	2400
		Unconfined strength	48 MPa
		Failure strain	0.1
Steel reinforcement	*MAT_PLASTIC_KINEMATIC (MAT_003)	Mass density	7800
		Young's modulus	230 GPa
		Poisson's ratio	0.3
		Yield stress	600 MPa
		Failure strain	0.2

For the steel reinforcement, the material model named *MAT_PLASTIC_KINEMATIC (MAT_003) is used. This material model is fitted for simulating isotropic and kinematic hardening plasticity with consideration of the rate effects [32]. The isotropic and kinematic hardening can be specified by varying the hardening parameter between 0 and 1. The Cowper–Symonds model is applied to account for its strain rate sensitivity under blast loading [19]. A strain rate dependent factor of $1 + (\dot{\varepsilon}/C)^{1/P}$ is used to scale the yield stress, where $\dot{\varepsilon}$ is the strain rate, C and P are the strain rate parameters, which are 40000 and 5.5, respectively in the current model. The material properties of the reinforcements used in the simulation are listed in Table 1.

2.2.3. Strain Rate Effects

When the reinforced concrete structures are subjected to blast loading or other high-speed impacts, both concrete and steel may respond at very high strain rate. In this situation, the inertia and strain rate effect are different from that of the quasi-static scenario. Therefore, a dynamic increase factor (DIF), the ratio of the dynamic-to-static material strengths versus strain rate, is considered to realize simulation of RC slab under blast loading. Definitions of DIF for compressive strength concrete, tensile strength concrete and steel reinforcement as follows.

The compressive strength of concrete can be determined by [32]:

$$\mathrm{CDIF} = \frac{f_c}{f_{cs}} = \begin{cases} \left(\dfrac{\varepsilon}{\varepsilon_{cs}}\right)^{1.026\alpha} & for\ \ \varepsilon \le 30\ \mathrm{s}^{-1} \\[4mm] \gamma_s \left(\dfrac{\varepsilon}{\varepsilon_{cs}}\right)^{1/3} & for\ \ \varepsilon > 30\ \mathrm{s}^{-1} \end{cases} \tag{4}$$

Where f_{cs} is the static compressive strength of concrete at strain rate ε_{cs}; f_c is the dynamic compressive strength at ε; ε_{cs} is the static strain rate of 30×10^{-6} s^{-1}; ε is the strain rate in the range of 30×10^{-6} to 300 s^{-1}; $\log \gamma_s = 6.156\alpha - 0.49$; $\alpha = 1/(5 + 3f_{cu}/4)$, f_{cu} is the static cube compressive strength in MPa.

The tensile strength of concrete is expressed by [33]:

$$\text{TDIF} = \frac{f_t}{f_{ts}} = \begin{cases} \left(\dfrac{\varepsilon}{\varepsilon_{ts}}\right)^{\delta} & for \ \varepsilon \le 1\,\text{s}^{-1} \\[3mm] \beta\left(\dfrac{\varepsilon}{\varepsilon_{ts}}\right)^{1/3} & for \ \varepsilon > 1\,\text{s}^{-1} \end{cases} \tag{5}$$

Where f_{ts} is the static tensile strength at strain rate ε_{ts}; f_t is the dynamic tensile strength at ε; ε_{ts} is the static strain rate in 10^{-6}s^{-1}; ε is the strain rate in the range of 10^{-6} to 160 s^{-1}; $log \ \beta = 6\delta\text{-}2$; $\delta = 1/(1+8f_{cs}/f_{co})$, f_{cs} is the static uniaxial compressive strength of concrete, $f_{co} = 10$ MPa.

For steel reinforcement, the dynamic increase factor (DIF) can be expressed as follows [34]:

$$\text{DIF} = \left(\frac{\varepsilon}{10^{-4}}\right)^{\alpha} \tag{6}$$

With the yield strength, $\alpha = \alpha_{fy}$ is expressed as follows:

$$\alpha = \alpha_{fy} = 0.074 - 0.04 f_y/414 \tag{7}$$

With the ultimate strength, $\alpha = \alpha_{fu}$ is expressed as follows:

$$\alpha = \alpha_{fu} = 0.019 - 0.009 f_y/414 \tag{8}$$

Where f_y is the yield stress in MPa (if f_y is in ksi, the 414 denominator should be replaced by 60), and the strain rate is in s^{-1}(1/second). It should be note that Equation 7 and 8 are valid with yield stresses between 290 and 710 MPa (42 and 103 ksi), and for strain rates between 10^{-4} s^{-1}and 10 s^{-1}.

Previous studies [35-37] showed that the above material properties could give reliable predictions of structural responses subjecting to blast loading, and it has been widely used for modeling RC structures especially for RC slabs.

2.2.4. Contact Formulation and Erosion Algorithm

Interaction between support plates and RC slab is modelled by a general contact algorithm, which uses a penalty contact method. This method searches for small nodal penetrations between surfaces where contact occurs. Algorithm *CONTACT_AUTOMATIC_SINGLE_SURFACE in LS-DYNA is used to simulate contact between the support plates and the RC slab. The algorithm generates master and slave surfaces automatically. The interface stiffness is computed as a function of the volume, bulk modulus and face area of the elements on the contact surface.

The erosion algorithm is used to simulate the concrete damages under the blast or impulsive loads, such as shear failure, cratering, spalling and crushing under blast loading and impact loading. The function *MAT_ADD_EROSION (MAT_22) in LS-DYNA is used to describe the physical damages of concrete under blast or impulsive loads. This function can smooth the simulation and simulate the element failure which is not defined for some solid element models in LS-DYNA. However, such erosion is irreversible, so an appropriate criteria need to be defined. In the previous study, the erosion algorithm has been widely used in simulating the dynamic response of concrete under blast loading [38-40]. Chen and Hao adopted an erosion criterion according to the principle strain of 0.1 to simulate the failure of concrete under blast loading [20]. Some other researchers used different erosion criteria to simulate the spall damage of different concrete materials [23, 41, 42]. In this study, the erosion criterion is set as 0.1 after intensive simulations which carried out with different erosion criteria, it is found that using principle tensile strain of 0.1 leads to reliable predictions of RC slab responses.

2.2.5. Application of Blast Loading

In this paper, blast loading is simulated with the *LOAD_BLAST function in LS-DYNA. This function is mainly based on empirical relations derived from blasting tests and is developed based on a report by Randers-Pehrson and Bannister [43], the load surface of the structure is clear. It has been proved to be reliable and widely used for the simulation of blast loading on structures [13, 22, 23]. The most advantage of this function is that the detailed modelling of explosive charge and shock wave propagation in air can be avoided, therefore it can save the computational burden. By using this function, a proper pressure history can be generated based on the inputs for an equivalent mass of TNT. Then the blast loading is propagated to the structure surface which searched by the pressure surface identification automatically. A termination time is set to ensure the explosive reaction is completely related to the concrete slabs. However, the influence of shapes for explosive charges on the response of structures under blast loading cannot be studied by this function. The interaction between shock wave and structure cannot be modelled, and the effect of clearing blast wave will be neglected, either.

2.3. Results and Comparisons

As aforementioned, the data reported by Sun [6] are used here for model calibration. In the simulating results, the average maximum deflection in the mid-span of the normal RC slab is 47.04 mm (See Figure 4), which is close to the experimental result (50.0 mm) with an error of around 5.9%. It indicates that the maximum deflection of the normal RC slab is well predicted by the finite element model.
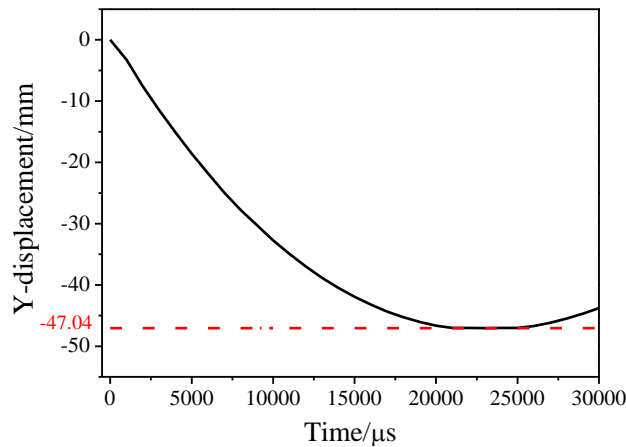

Figure 4. The mid-span deflection of numerical results for normal RC slab

The comparison of damage distributions on the bottom surface of normal RC slab obtained from blast test and numerical simulation are shown in Figure 5, the plastic strain distribution of the slab is considered to be the simulation result. As illustrated in Figure 5a, steel reinforcement is exposed in the centre on the bottom surface of the slab, concrete with spall damage and RC slab with some extensive cracks are obviously. In the numerical simulation study, the numerically simulated plastic strain contour is shown for comparison. As shown in Figure 5b, the phenomenon of steel bar exposed the bottom surface and the concrete with spall damage are well captured, major cracks in the RC slab are also reasonably reproduced. From the above analysis, the numerical simulation well captures the damage distributions of the RC slabs.

Therefore, comparing with the experimental study, it can be seen that the established numerical model can lead to reasonable predictions of the structural response for the cracked RC slab under blast loading.
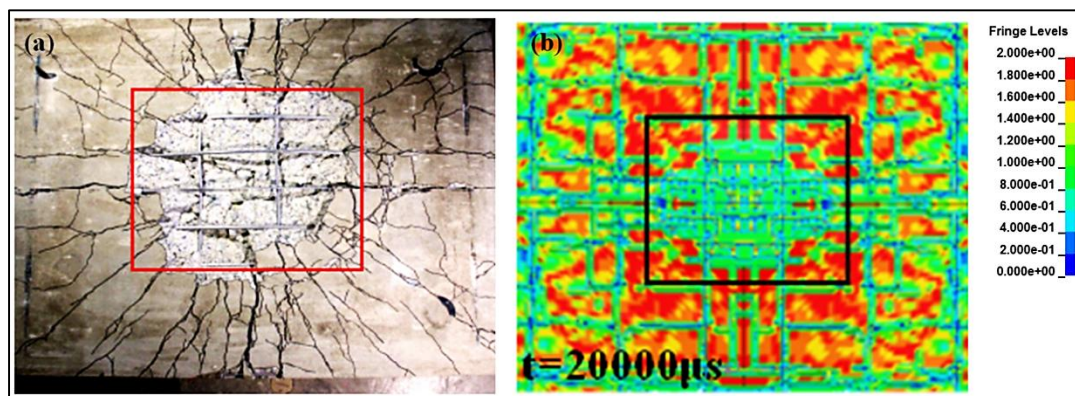

Figure 5. Comparison of the numerical and experimental results for normal RC slab: (a) experimental results on the bottom surface [6], (b) numerical results on the bottom surface

3. Numerical Simulation

The above calibrated numerical model is used in the following study to perform a series of simulations of cracked RC slabs under blast loading. The structural responses such as the damage distributions and the mid-span deflection are compared with that of the normal RC slab to examine the blast resistance of the cracked RC slabs. The influence of different crack parameters, such as crack orientations, widths and depths to mention a few, on the failure characteristics of cracked slabs are also investigated.

3.1. Finite Element Model of the Cracked RC Slab

Herein, the objective is to model the slab with an "initial crack" in the centre of the bottom surface under blast loading. Comparing with the normal RC slab, numerical simulations are conducted to study the dynamic performance and failure behaviour of the cracked RC slab. Having the actual dimensional sizes, boundary conditions, concrete material properties and reinforcement confinements, the cracked RC slab model is developed based on the normal RC slab. Three different orientations (0°, 45° and 90°), widths (1, 2 and 3 mm) and depths (20, 25 and 30 mm) are taken into consideration. The singular elements [44] are used to create a special mesh around the cracks to solve the stress concentrations deriving from the crack tip. Details of mesh at the crack tip are shown in Figure 6.
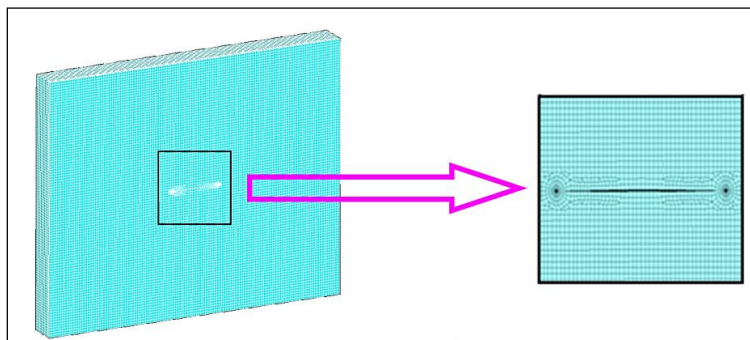

Figure 6. Details of mesh at the crack tip for the model

Figure 7 shows the damaged results at various stages on the top and bottom surfaces of the cracked slab during the analysis for the model with the crack at 0°. The cracked model has the initial crack with length of 200 mm, width of 2 mm, and depth of 20 mm. As can be seen in Figure 7, the maximum strain first occurs at the central of the bottom surface since it subject to tensile stress in the blast loading, and the damage initiates from the initial crack tip, then it propagates quickly with cracks found in the support areas (constrained edges) on the top surface due to the punching shear stress. On the top surface of the RC slab (see Figure 7a), cracks are mainly formed in the support areas with some minor cracks around the initial crack in the centre of the slab. On the bottom surface of the RC slab (see Figure 7b), an obvious spall damage area is observed at the centre with a large number of major cracks been developed along the horizontal direction. Besides, cracks along the vertical and 45° directions are also found. Comparison with the damage destruction on the bottom surface of normal cracked RC slab as shown in Figure 5, it can be seen that the damage phenomena of the normal cracked RC slab is similar to that of the cracked RC slab. However, the level of damage of the cracked RC slab is much more serious. For example, at the same time t=20000 μs, significantly larger spall damage area and more cracking are occurred in the bottom surface of the cracked slab.
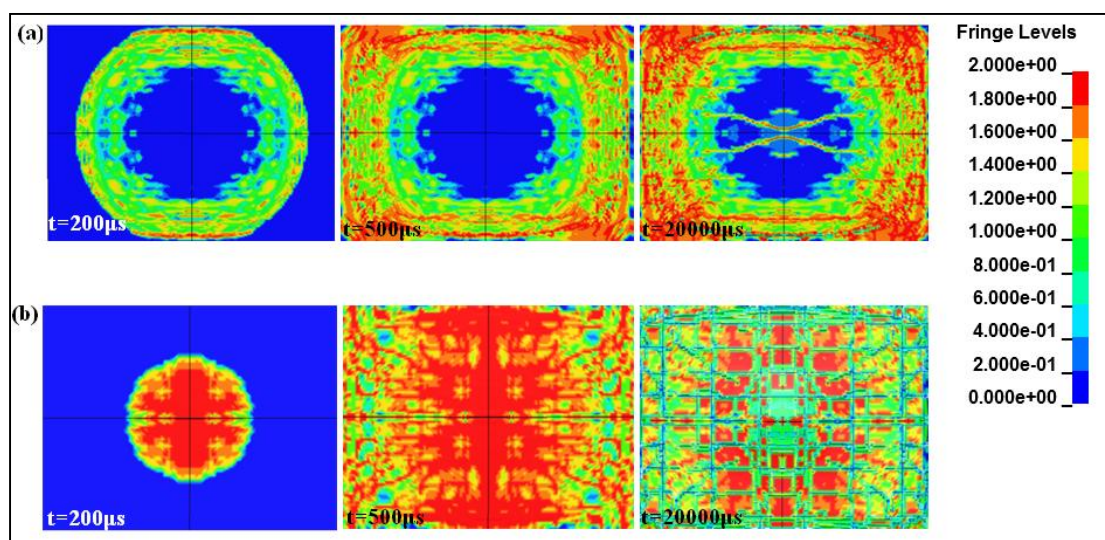

Figure 7. Damage distributions on the (a) top and (b) bottom surfaces of a RC slab with a crack (0o) in the middle of the bottom surface

Figure 8 shows the comparison of the von Mises stress contours between the cracked RC slab (Figure 8a) and normal slab (Figure 8b) in the cross section at different times under blast loading. The red color indicates the greater stress. In general, the larger the internal stress is, the easier it is to be damaged. Through the comparison and analysis, we find that the damage behaviour of the cracked slab is similar to that in the normal slab, but the damage process is a

bit different. For example, at the time of 190 *μs*, it is clear that red area in the cross section of the cracked RC slab is obviously greater than that of the normal RC slab, which means the cracked slab in this section bears greater stress. From 190 to 200 *μs*, for the slab with initial crack, the scope of the stress wave is increased significantly and the maximum stress is quickly spread to the junction of steel and concrete from the center of the slab. This shows that the shock wave quickly destroys the concrete near the crack tip within 10 *μs*. Meanwhile, for the normal slab without initial crack, the increasement scope of the stress wave is obviously smaller than the cracked RC slab in the same period. When the time reaches 500 *μs*, there is an obvious damage area around the tip of the initial crack in the bottom surface of the cracked slab, while not yet found in the normal RC slab. This means the cracked RC slab shows similar damage behaviour as the normal RC slab, but with an early reaction. In addition, when the time arrivals 20000 *μs*, from the comparison of the von Mises stress contours showed in the Figure 8, we can also see that the damage degree of the cracked RC slab looks more serious than that in the normal slab, the result is consistent with the above analysis based on the plastic strain contours as shown in Figure 7.

Figure 9 illustrates the comparison of displacement history curves of mid-span for both the cracked and normal RC slabs. As can be seen, the displacement history behaviour of the cracked slab is similar to that of the normal model. However, the maximum deflection and the failure time are different. The maximum deflection of the cracked RC slab is 55.59 mm, with an increase of around 18.2% in the deformation compared with the normal model (the maximum deflection value is 47.04 mm). This also indicates that the RC slab with initial crack experienced more serious damage than the normal RC slab. Corresponding to the maximum deflection shown in Figure 9, we can also see that the failure time of normal RC slab at the bottom surface is around 20000 *μs*, while that of the cracked one is ~28000 *μs*. This shows that, corresponding with the analysis of the above section, an initial crack in RC slab will cause earlier damage than the normal RC slab.
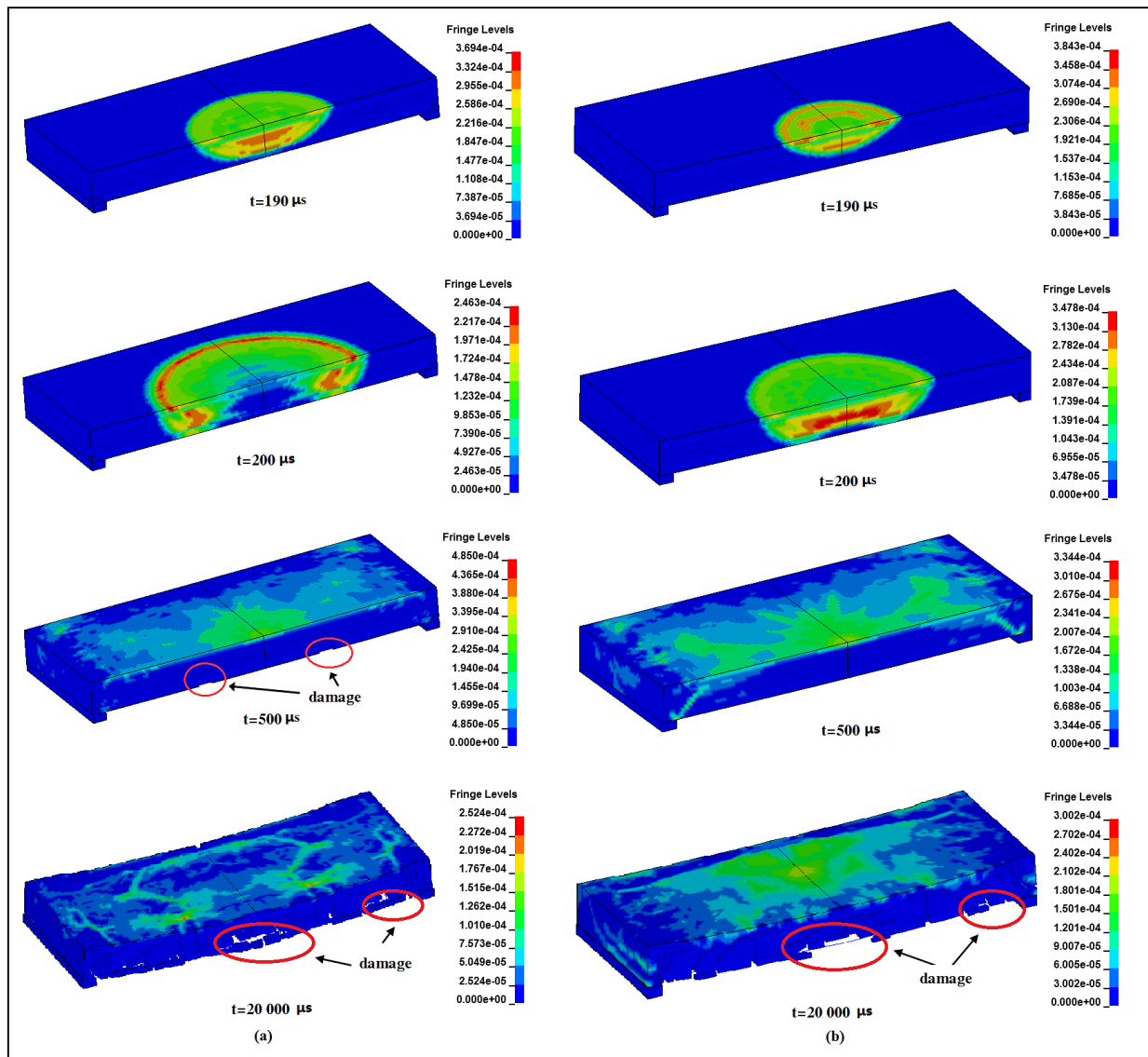

Figure 8. Von Mises Stress contours at different times: (a) cracked RC slab with a crack length of 200 mm, crack width of 2 mm, crack depth of 20 mm, crack orientation of 0°; (b) normal RC slab
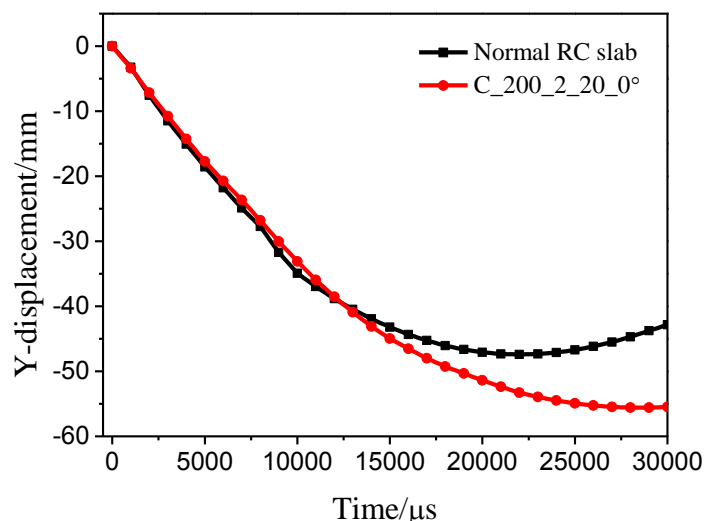
Figure 9. Displacement history curves of mid-span node of RC slab with or without cracks

3.2. Influence of Crack Orientation

In order to study the influence of crack orientation on the dynamic behaviour of cracked RC slab, models of three typical different crack orientations (0º, 45º, and 90º) in RC slab are established, as shown in Figure 10. The rest parameters of the cracks in RC slab are given as follows: length 200 mm, width 2 mm, and depth 20 mm, and centres of them are coincident with the centre bottom faces of the slab. It is noteworthy that crack direction in the actual reinforced concrete slab is arbitrary and changeable. We will study this effect in a very near future.
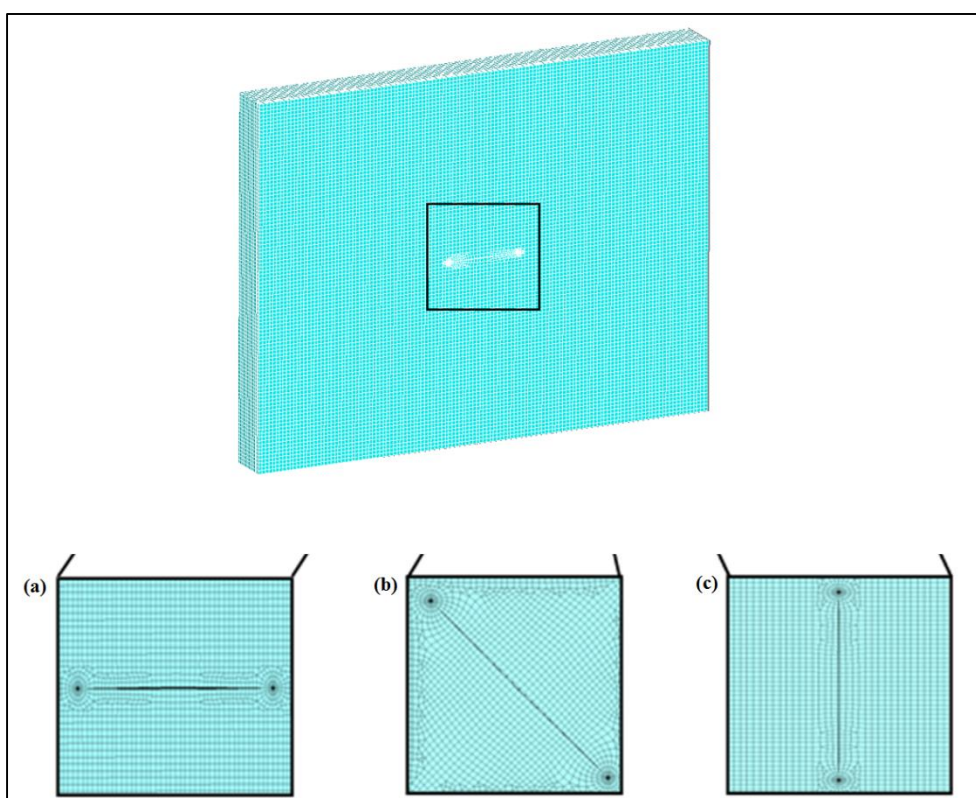

Figure 10. Models of three typical different crack orientations: (a) crack at 0°; (b) crack at 45°and (c) crack at 90°

Figure 11 shows the comparisons of mid-span displacement time histories for the RC slabs with different crack orientations (0º, 45º and 90º). From the curves, it can be seen that for the cracked slabs with different crack orientations, the displacement history behaviour shows similar features, and there is no significant difference in their maximum deflection from a macro perspective. For example, with initial cracks along the horizontal (0º) and vertical (90º) directions, the maximum deflections of the cracked slabs are about 55.25 mm and 55.92 mm, respectively. This

slight difference may be caused by the reason that the slab model in this paper is not square, but a rectangle. The length of the long side is 1300 mm, while that of the short side is 1000 mm. When the initial crack orients an angle of 90°, it means the direction of the crack is the same with the short side (see Figure 10). In this case, the shock wave is easier to reach the edge of the short side of slab, and the concrete is prone to damage at the end of the short side due to the change of propagation medium. This will make the damage of the cracked RC slab with a crack orientation of 90° slightly more serious than that of the model with a crack orientation of 0°.
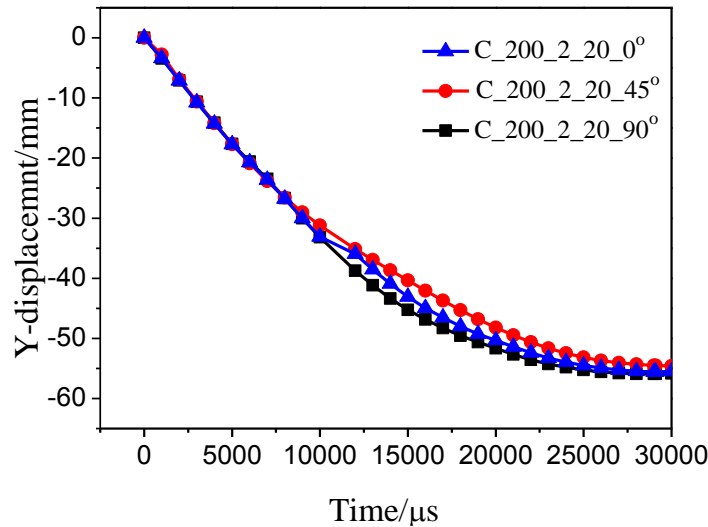

Figure 11. Mid-span deflection time histories of cracked RC slab with three crack orientations (0°, 45°, 90°) under blast loading

3.3. Influence of Crack Width

Three different cracked RC slabs with crack width of 1, 2, and 3 mm are modelled under the same length (200 mm), depth (20 mm) and orientation (0°) to study the influence of crack width in the RC slab under blast loading. The time history curves of mid-span deflections of these RC slabs with different width are shown in Figure 12. It can be seen that, similar to the influences of the crack orientations, all three crack models present a similar time history curves. As the crack width increases, the maximum deflection of the cracked models will also slightly increase. For example, the maximum value of deflection only increase 3.7% from 53.08 to 55.60 mm when the width of the initial crack increases from 1 to 3 mm. This indicates that the dynamic performance of cracked RC slabs in the given situations is insensitive to the minor crack widths.
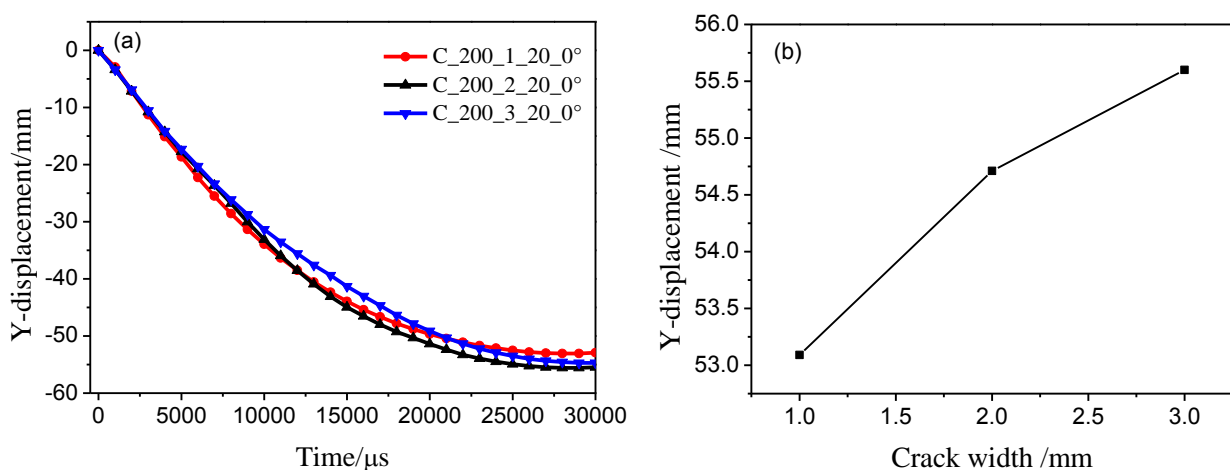

Figure 12. Mid-span deflection time histories of cracked RC slab with three crack widths (1, 2 and 3 mm) under blast loading: (a) mid-span deflection time histories of RC slab; (b) maximum deflection of cracked RC slab in different crack widths

3.4. Influence of Crack Depth

In this section, cracked RC slabs having the same length (200 mm), width (2 mm) and orientation (0°) but with different crack depths of 20, 25 and 30 mm are modelled. The damage distributions of these cracked RC slabs under

blast loading are applied, and the time history curves of mid-span deflection are presented in Figure 13. It is apparent that all three crack models present a similar time history curves. However, as expected, the maximum deflection does not increase with the increase of the crack depth. The maximum value of deflection (57.52 mm) occurs when the crack depth is 25 mm in the three sets of simulation experiments. Similar to the previous results, initial crack depth has little influence on the damage of RC slab under this blast loading.
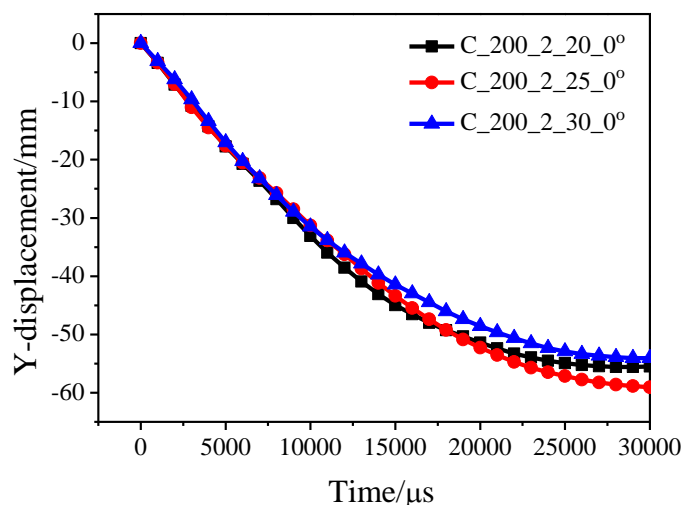

Figure 13. Mid-span deflection time histories of cracked RC slab with three crack depths (20 mm, 25 mm, 30 mm) under blast loading

4. Conclusion

In this paper, a Lagrange strain damage finite element analysis is successfully performed to simulate the dynamic behaviour of cracked RC slabs subjected to blast loading. Characteristics of the strain, stress and displacement during the blast loading of cracked RC slabs are presented. The computed damage distribution and maximum deflection of normal specimens are first compared with experimental tests to give a calibration of the established numerical model, the basic consistent damage distribution and the small difference (5.9%) of the maximum deflection between the simulation and test results indicate that the dynamic behaviour of the RC slabs under the blast loading can be well predicted by the established model.

After proper calibration, the dynamic distribution of RC slab with initial crack is identified. It is shown that the damage of the cracked slab initiates from the initial crack tip of the bottom surface, and then it propagates quickly with cracks found in the support areas (constrained edges) on the top surface. The existence of initial crack in the RC slab makes it experience more serious damage than the normal RC slab under the same explosive loads, as well as an early reacted failure time. The maximum deflection of the cracked RC slab is 55.59 mm, with an increase of around 18.2% in the deformation compared with that of the normal model which has a maximum deflection value of 47.04 mm. In succession, based on the above analysis, influences of crack orientation, width and depth on the dynamic behaviour of the cracked RC slabs under the blast loading are further investigated. The simulation results show that different crack parameters have certain influences on the dynamic behaviour of cracked RC slabs, but the effects are not significant.

This paper presents an alternative method for modelling RC slab behaviour. The promising part is that dynamic response of RC slab under blast loading can be modelled. However, the conclusions obtained are solely based on illustrative analysis of the simple numerical examples in this study. In practical engineering, cracks in the RC slab are formed in the casting process or propagated from the original cracks in use, the locations and sizes of cracks are different from than that of man-made in the specimen. Therefore, conclusions may not be generalized immediately, especially when the width and depth of initial cracks on the RC slab are larger than 3 and 30 mm, respectively. Furthermore, bond slip between steel bar and concrete are assumed to be perfect which not the same as actual are. Hence, requirements for more robust and accurate numerical algorithms are needed.

5. Acknowledgments

6. References

[1] Liu B., Villavicencio R., Soares G.C. "Experimental and numerical plastic response and failure of pre-notched transversely impacted beams." International Journal of Mechanical Sciences77(2013): 314–319, https://doi.org/10.1016/j.ijmecsci.2013.09.032.

[2] Feng P., Hu L.L., Zhao X.L., Cheng L., Xu S.H. "Study on thermal effects on fatigue behavior of cracked steel plates strengthened by CFRP sheets." Thin-Walled Structures 82 (2014): 311–320, https://doi.org/10.1016/j.tws.2014.04.015.

[3] Brighenti, R. "Numerical buckling analysis of compressed or tensioned cracked." Engineering Structures 27.2 (2005): 265–276, https://doi.org/10.1016/j.engstruct.2004.10.006.

[4] Razaqpur, A.G., Tolba, A., Contestabile, E. "Blast loading response of reinforced concrete panels

reinforced with externally bonded GFRP laminates." Compos Part B: Eng 38 (2007) :535–546, https://doi.org/10.1016/j.compositesb.2006.06.016.

[5] Mays G.C., Hetherington J.G., Rose T.A. "Response to blast loading of concrete wall panels with openings." J Struct Eng 125.12 (1999): 1448–1450, https://doi.org/10.1061/(ASCE)0733-9445(1999)125:12(1448).

[6] Sun W.B. "Experimental studies on reinforced concrete (RC) slabs subjected to blast loads." Journal of Liaoning Technical University 28.2 (2009): 217–220. (In Chinese).

[7] Lok T.S., Xiao J.R. "Steel-fibre-reinforced concrete panels exposed to air blast loading." Proc ICE-Struct Build 134 (1999):319–331.

[8] Chi Y., Langdon G.S., Nurick G.N. "The influence of core height and face plate thickness on the response of honeycomb sandwich panels subjected to blast loading." Mat Des 31 (2010) :1887–1899, https://DOI: 10.1016/j.matdes.2009.10.058.

[9] Xu K., Lu Y. "Numerical simulation study of spallation in reinforced concrete plates subjected to blast loading." Comput Struct 84.5 (2006):431–437, https://doi.org/10.1016/j.compstruc.2005.09.029.

[10] Yuan L., Gong S.F., Jin W.L. "Spallation mechanism of RC slabs under contact detonation." Trans Tianjin Univ 14.6 (2008):464–473. (In Chinese).

[11] Tai Y.S., Chu T.L., Hu H.T., Wu J.Y. "Dynamic response of a reinforced concrete slab subjected to air blast load." Thero Appl Fract Mec 56.3 (2011):140–146, https://doi.org/10.1016/j.tafmec.2011.11.002.

[12] Zhao C.F., Chen J.Y. "Damage mechanism and mode of square reinforced concrete slab subjected to blast loading." Theoretical and Applied Fracture Mechanics 63 (2013):54–62, https://doi.org/10.1016/j.tafmec.2013.03.006.

[13] Lin X.S., Zhang Y.X., Hazell P.J. "Modelling the response of reinforced concrete panels under blast loading." Mater Des 56.1 (2014):620–627, https://DOI:10.1016/j.matdes.2013.11.069

[14] Wang W., Zhang D., Lu F.Y., Wang S.C., Tang F.J. "Experimental study on scaling the explosion resistance of a one-way square reinforced concrete slab under a close-in blast loading." Int J Impact Eng 49 (2012):158–164, https://doi.org/10.1016/j.ijimpeng.2012.03.010.

[15] Brighenti, R. "Influence of a central straight crack on the buckling behaviour of thin plates under tension, compression or shear loading." Int J Mech Mater Des 6.15 (2010):73–87. https://DOI:10.1007/s10999-010-9122-6.

[16] Paik J.K., Satish Kumar Y.V., Lee J.M. "Ultimate strength of cracked plate elements under axial compression or tension." Thin-Walled Struct 43.2 (2005):237–272, https://doi.org/10.1016/j.tws.2004.07.010.

[17] Hao J.B., Li X.D., Mu Z.T. "Fatigue behavior of thick center cracked aluminum plates repaired by two-sided composite patching." Materials and Design 88 (2015):331–335, https://DOI:10.1016/j.matdes.2015.09.011

[18] Alinnia M.M., Hosseinzadeh S.A.A., Habashi H.R. "Numerical modelling for buckling analysis of cracked shear panels." Thin-Walled Structures 45.12 (2007):1058–1067, https://doi.org/10.1016/j.tws.2007.07.004.

[19] LS-DYNA. LS-DYNA keyword user's manual. version 971. Livermore Software Technology Corporation, Livermore, California, L.C., 2007.

[20] Chen, W.S., Hao, H., Chen, S.Y. "Numerical analysis of prestressed reinforced concrete beam subjected to blast loading." Materials and Design 65 (2015): 662–674, https://doi.org/10.1016/j.matdes.2014.09.033.

[21] Yao S.J., Zhang D., Chen X.G., Lu F.Y., Wang W. "Experimental and numerical study on the dynamic response of RC slabs under blast loading." Engineering Failure Analysis 66 (2016): 120–129, https://doi.org/10.1016/j.engfailanal.2016.04.027.

[22] Lin X.S., Zhang Y.X.. "Nonlinear Finite Element Analysis of FRP-Strengthened Reinforced Concrete Panels Under Blast Loads." International Journal of Computational Methods 13 (2016) :1641002–1–17, http:// DOI: 10.1142/S0219876216410024 .

[23] Qu Y.D., Li X., Kong X.Q., Zhang W.J., Wang X.Z.. "Numerical simulation on dynamic behavior of reinforced concrete beam with initial cracks subjected to air blast loading." Engineering Structures 128 (2016) :96–110, http://dx.doi.org/10.1016/j.engstruct.2016.09.032.

[24] Tu Z., Lu Y. "Evaluation of typical concrete material models used in hydrocodes for high dynamic response simulations." Int J Impact Eng 36(2009):132–146, https://DOI:10.1016/j.ijimpeng.2007.12.010.

[25] Malvar L.J., Morrill K.B., Crawford J.E. "Numerical modeling of concrete confined by fiber-reinforced composites." Journal of Composites for Construction 8 (2004):315–322, https://DOI:10.1016/(ASCE)1090-0268(2004)8:4(315).

[26] Magallanes J.M., Wu Y., Malvar L.J., Crawford J.E. "Recent improvements to release III of the K&C concrete model." In the 11th international LS-DYNA users conference, 2010.

[27] Li J., Hao, H. "Influence of brittle shear damage on accuracy of the two-step method in prediction of structural response to blast loads." International Journal of Impact Engineering 54 (2013):217–231, https://doi.org/10.1016/j.ijimpeng.2012.11.008.

[28] Malvar L.J., Crawford J.E., Wesevich J.W., Simons D. "A plasticity concrete material model for DYNA3D." International Journal Impact Engineering 19.9–10 (1997):847-873, https://doi.org/10.1016/S0734-743X(97)00023-7.

[29] Pan J.L., Zhou J.J., Luo M. "Numerical simulations on dynamic responses of FRP strengthened reinforced concrete two-way slabs under blasting loading." Journal of PLA University of Science and Technology 12.6 (2011): 643–648. (In Chinese).

[30] Yao, S.J., Zhang, D., Chen, X.G., Lu, F.Y., Wang, W. "Experimental and numerical study on the dynamic response of RC slabs under blast loading." Engineering Failure Analysis 66 (2016): 120–129, https://doi.org/10.1016/j.engfailanal.2016.04.027.

[31] Shi Y.C., Hao H., Li Z.X. "Numerical derivation of pressure–impulse diagrams for prediction of RC column damage to blast loads." International Journal Impact Engineering 35.11 (2008):1213–1227, https://DOI:10.1016/j.ijimpeng.2007.09.001

[32] Beton CE-Id. "Concrete structures under impact and impulsive loading." CEB Bull 1990:187.

[33] Malvar L.J., Ross C. A. "Review of strain rate effect for concrete in tension." ACI Mater J 96.5 (1999) :614–616.

[34] Malvar L.J. "Review of static and dynamic properties of steel reinforcing bars." ACI Mater J 95.5 (1998): 609–616.

[35] Xu K., Lu Y. "Numerical simulation study of spallation in reinforced concrete plates subjected to blast loading." Computers Structures 84.5-6 (2006): 431–438, https://doi.org/10.1016/j.compstruc.2005.09.029.

[36] Hudson J.L., Darwin D. "Evaluation and repair of blast damaged reinforced concrete beams." A Report on Research Sponsored by the University of Kansas, Structural Engineering and Materials Laboratory, USA, 2005.

[37] Yang J. L., Zhang Y., Yu T.X. "An experimental study of imperfect clamped beams subjected to impact." Explosion Shock Waves 12.1 (1992): 22–29. (In Chinese).

[38] Coughlin A.M., Musselman E., Schokker A.J., Linzell D. "Behavior of portable fiber reinforced concrete vehicle barriers subject to blasts from contact charges." International Journal of Impact Engineering 37.5(2010):521–529, https://DOI:10.1016/j.ijimpeng.2009.11.004.

[39] Tang E.K., Hao H. "Numerical simulation of a cable-stayed bridge response to blast loads, Part I: model development and response calculations." Engineering Structure 32.10(2010):3180–3192, http:// doi.org/10.1016/j.engstruct.2010.06.007.

[40] Wu K.C., Li B., Tsai K.C. "The effects of explosive mass ratio on residual compressive capacity of contact blast damaged composite columns." Journal of Constructional Steel Research 67.4(2011):602–612, http:// doi.org/10.1016/j.jcsr.2010.12.001.

[41] Li J., Hao H. "Numerical study of concrete spall damage to blast loads." International Journal of Impact Engineering 68 (2014) 41–55, http://dx.doi.org/10.1016/j.ijimpeng.2014.02.001.

[42] Gong S.F., Deng H., Zhu S.B., Jin W.L. "Numerical simulation for dynamic failure of a reinforced concrete slab under close-in-explosion." Journal of Vibration and Shock 31.2(2012):20–24,100. (In Chinese)

[43] Randers-Pehrson G., Bannister K.A. "Air blast loading model for DYNA2D andDYNA3D ARL-TR-1310." Adelphi MD: Laboratory AR., Ed. USA, 1997.

[44] Pereira J.M., Ghasemnejad H., Wen J.X., Tam V.H.Y. "Blast response of cracked steel box structures repaired with carbon fibre-reinforced polymer composite patch." Materials and Design 32.5 (2011):3092–3098. https://DOI:10.1016/j.matdes.2010.12.045.